Pedestrian Shoulder and Spine Kinematics in Full-Scale PMHS Tests for Human Body Model Evaluation

Ruth Paas[1], Johan Davidsson[1], Catherine Masson[2], Ulrich Sander[1, 3], Karin Brolin[1], Jikuang Yang[1]

[1] Faculty of Applied Mechanics, Chalmers University of Technology, Gothenburg, Sweden
[2] French Institute of Science and Technology devoted to Transport, Planning and Networks (IFSTTAR), France
[3] Autoliv Research, Sweden

Abstract   Tools such as human body models are required to show the benefit of restraints needed to reduce risk of injuries and fatalities for pedestrians. To assess the biofidelity of these tools, representative, detailed validation data are required.

One aim was to investigate shoulder and spine response in pedestrian/vehicle collisions by analysing new and existing post mortem human subject (PMHS) full-scale tests. Furthermore, assessment was performed whether the specific loading conditions in these PMHS tests were similar to existing component tests and representative of real-life accidents.

A full-scale PMHS test was conducted for detailed 6DOF analysis, and three tests were re-analysed. The hands were not tied together in any of the tests, different leg positions were used. To compare loading conditions with real life, accident data was analysed.

Beginning with pelvis impact, the spine was drawn inferiorly while the head rotated contralaterally. Before elbow-to-vehicle contact, the ipsilateral scapula rotated upwards, elevated and adducted. Following elbow contact it elevated rapidly until shoulder-to-vehicle impact. Elbow contact appeared to affect the thorax and head kinematics; the head rotated towards the vehicle worsening the head impact. The results underline the necessity to collect additional 6DOF elbow, scapula and spine data in full-scale pedestrian impacts.

Keywords   Kinematics, Pedestrian, PMHS, Shoulder, Spine

I.   INTRODUCTION

Statistics indicate that pedestrian safety is still an issue, and that additional research is required to reduce pedestrian accidents and the risk of associated injuries [1]-[6], [17]. A key issue in preventing fatalities and injuries during a pedestrian accident is a large scale introduction of restraints with documented benefits, requiring validated test tools. Both the development of these restraints and the validation require a sound understanding of pedestrian kinematics.

Overall, pedestrian kinematics has predominantly been studied using PMHSs. Such tests and component tests, i.e., tests carried out on specific body parts, are the main data source for validation of test tools such as Human Body models (HBMs). It is, however, sometimes difficult to assess the relevance of a specific body part test for validation of a pedestrian HBMs, as the impact boundary conditions may vary considerably between those in a full-scale test or to those common in real-life accidents. Kinematics in full-scale pedestrian testing has proved to be very sensitive to the initial conditions. This is one of the reasons why most full-scale pedestrian tests are conducted in what is known as a standard test set-up, in where the test subject is impacted laterally and hits the middle of the vehicle front. Furthermore, to achieve enhanced repeatability the subject's hands are sometimes tied together. The issue of the initial condition may be a reason why pedestrian testing is often performed with impactors such as flex legs and head forms. Compared to the real world, the standard set-up represents only a limited proportion of the pedestrian accidents. Additional validation data would be valuable for the development of humanlike pedestrian HBMs.

The majority of full-scale PMHS pedestrian tests have investigated two dimensional kinematics of the head, spine or legs [7]-[14] and have to some degree made data available for HBM validation. Data sets have primarily been limited to displacements in two dimensions. More recently, attempts have been made to assess head rotation [15], as its rotational acceleration may increase the risk of brain injuries. Rotation of other body regions

has been poorly addressed, especially rotation other than in the coronal plane. However, since human joints are not equally flexible in all directions, overall body rotation in the transverse plane may change the effective stiffness in joints such as the hip or the spine joints. Joint properties play an essential role in defining how impact energy propagates through the body. In the case of pedestrian impacts, they determine how the impact energy is transferred from the leg and pelvis to the upper body, and further to the head-neck complex. Thus, rotation influences the overall body kinematics and consequently contributes to defining the boundary conditions of head impact on the vehicle. Displacements of the arms and shoulders in pedestrian impacts are not reported, even though the arms may influence head-to-vehicle contact conditions. Hence, there is a need for additional pedestrian HBM validation data with particular focus on joint angulations, and elbow and shoulder motions.

Therefore, this paper aims to provide 6DOF data for the head, spine and shoulder in pedestrian-to-vehicle tests. It investigates the influence of elbow and shoulder impact on the thorax and head kinematics, and compares these boundary conditions to impactor tests and real life accidents. For this purpose, a new analysis of accident data addressing shoulder and elbow impacts is presented.

II. METHODS

One full-scale pedestrian PMHS experiment (FSR02) was conducted, and three previous PMHS tests (H1, H2, H3, [16]) have been re-analysed for this article.

Full-scale pedestrian PMHS experiment (FSR02)

The subject in experiment FSR02 was obtained and treated in accordance with guidelines for PMHS testing and permission was granted by the Ethical Committee of the Marseille Faculty of Medicine. The subject was impacted laterally by a small size sedan car at a velocity of 40 km/h. The subject was in a walking position with its contralateral leg slightly to the front and its ipsilateral leg slightly behind the centre of gravity (Fig. C3 in Appendix C). The subject had a stature of 172 cm, weighted 69 kg and was 72 years old. Preservation was a combination of refrigeration and Winkler's embalmment [18], and then storage at +4 to +6°C until testing. Prior to the experiment, the subject was screened for fractures and other pathologies to avoid test result interferences. The subject was attached to the ceiling with an electro magnet which was connected by four cable wires to a belt around the subject's neck. There was no mechanism installed to catch the subject before ground impact since injury investigation was not intended.

The vehicle was a recent model small sedan; its centreline is shown in Fig. 1, including the Bonnet Leading Edge (BLE) as defined by [19]. No parts were removed from the vehicle prior to the test. A coordinate system displaying the centreline offsets and Wrap Around Distances (WAD) was painted on the vehicle front. During the test the vehicle was accelerated to the target velocity. Ten milliseconds before the impact, the vehicle passed a light trap which was used to measure the impact velocity and start the countdown for releasing the PMHS from its attachment at the time of impact. 10 ms after the first contact, the vehicle's braking system was activated, inducing realistic break pitch.

Preparation of the subject began the day before the test. Aluminium plates of 70 x 70 x 3 mm were firmly fastened to both scapulae and to the T2, T11 and L4 vertebrae, using two or three screws per plate, as carriers for the photo targets. The plates were fixed to the scapulae via three cylindrical legs, each with a length of 45 mm. The construction maintained a distance between the bone and the plate and enabled the soft tissue in the region to move freely. The plates fixed to the vertebrae were attached with screws positioned immediately next to the vertebral process on the left and on the right side. The stature of the subject was measured once again in the hanging position immediately before the test, to confirm that it did not differ from the stature when horizontal.

A high-speed video camera (Redlake, N4, 2000 fps, 50 mm lens) was placed at a distance of 4.9 m from the impact point. The camera was facing the subject's posterior, focused on the subject's upper body, and was triggered by a contact switch mounted to the bumper. Three high speed cameras were facing the subject's anterior. One of them was placed on the ground at a distance of 6.5 m. The other two were mounted on the right side of the vehicle, one towards the outer edge of the windshield at head impact level and the other on the right-hand side front part of the roof. Spray paint was applied to the ipsilateral side of the pelvis, shoulder and the head immediately before the test so that the impact locations could be determined.
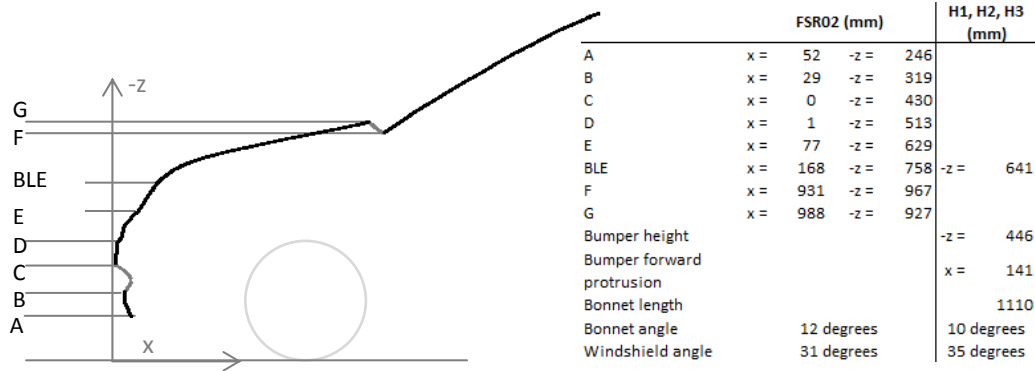
	FSR02 (mm)			H1, H2, H3 (mm)
A	x = 52	-z =	246	
B	x = 29	-z =	319	
C	x = 0	-z =	430	
D	x = 1	-z =	513	
E	x = 77	-z =	629	
BLE	x = 168	-z =	758	-z = 641
F	x = 931	-z =	967	
G	x = 988	-z =	927	
Bumper height				-z = 446
Bumper forward protrusion				x = 141
Bonnet length				1110
Bonnet angle		12 degrees		10 degrees
Windshield angle		31 degrees		35 degrees

Fig. 1. Vehicle centreline measurements with datum lines

6DOF video analysis was performed using TEMA Automotive 6D. In brief, the software converts perspective displacement of a film target group into 3D translations and 3D rotations of the body part that the target group is attached to. The targets in each group must be attached to a rigid surface, and the initial position of the targets relative to the camera and relative to a chosen reference point must be known. A calibration target is used for lens calibration and rotating this target enables a perspective calibration. This procedure makes it possible to quantify 3D lengths and 3D angulations as successive Euler rotations, calculated from perspective displacement of the targets in each target group. Here, the different reference point positions relative to the film target groups were measured by the assistance of a sketch of a 50 percentile male that provided body part centres. As a result, translation and rotation was obtained for the Centre of Gravity (CG) of the head, the scapula and in the bodies of T2, T11 and L4. The results were verified through visual inspection of the films captured by the other cameras.

The reference coordinate system was based on the vehicle coordinate system before impact (Fig. A2). Links were defined as straight lines between two targets, such that the head and T2 targets defined the neck link, the T2 and T11 targets defined the thorax link and the T2 and scapula targets defined the T2-to-scapula link. Link angles refer to the angulation of these lines relative to the stationary coordinate system, where zero degrees correspond to a vertical link. Positive angulation is equivalent to rotation towards the vehicle around the y-axis, or rotation in direction of negative pitch. Link lengths and angles were calculated to provide an estimate of relative body part positions (Fig. A2).

Reanalysis of previous PMHS tests

The tests were carried out in the late 1990's with a small sedan, modern at the time. A detailed methodology description for the H1, H2 and H3 tests can be found in [16]; the coordinate system was redefined for consistency with FSR02. In brief, the vehicle impacted the PMHS at 30 km/h (test H1) and 40 km/h (tests H2, H3). The ipsilateral leg was positioned slightly behind the centre of gravity. The PMHS details are summarised in Table I.

TABLE I AS IN [16]

PMHS DATA FOR TESTS H1, H2, H3

Experiment	H1	H2	H3
Stature [cm]	167	182	177
Mass [kg]	68	63	84
Gender	Male	Male	Male
Age at time of death	70	51	66

Film targets were attached with screws to the head and to three locations along the spine. The height at which they were attached was measured when the PMHS were in a horizontal position; the exact vertebrae they were attached to are unknown. It is estimated that the targets were attached to T1, T8 and to the sacrum. The vehicle, which was mounted to a sled system and had all parts under the bonnet removed, was decelerated at first contact with the PMHS. A ceiling-mounted electromagnet, which held the head at the desired height by metal cables, was released when the vehicle front was 0.5 m away from the PMHS. Secondary impact with the ground was avoided in order to allow for an investigation of the vehicle contact induced injuries only.

Three cameras recorded the collision; all were stationary and captured the posterior of the PMHS. The first camera was focused on the upper body, approximately from the pelvis to the head, the second was focused on

the lower body, from the feet to the lower end of the thorax; the third camera captured the full experiment. Film analysis was carried out on the film of the upper body. The coordinate system used is shown in Fig. A2.

The re-analysis of these tests was performed by using data published in [16]. Any information not available in the publication was additionally requested from one of the co-authors of the study. The aim of the re-analysis was to investigate the curvature of the spine by means of observing link angles. In order to estimate head rotations, the single head photo target related to the centre of the head area and other visual information were used. Links were defined using the same method as in the FSR02 test, although the neck link was defined using the T1 target and the head centre of area. In addition, comparison of shoulder and spine behaviour between the experiment in [16] and the observations in test FSR02 was performed.

Coordinate system

The coordinate system used is schematically presented in Fig. A2 in Appendix A. Estimation of lumbar, thorax and neck angular displacements was carried out using the links as shown in Fig. A2 in Appendix A. Where these links were used, all motion was projected into video plane.

Accident data

Estimates of shoulder and elbow impact frequencies in real-life accidents were investigated using German In-Depth Accident Study (GIDAS) [20] accident data from 1999-2011. Only accidents where pedestrians were hit by the front of a passenger car and where the pedestrian was not lying on the ground were included. The cases have not been weighted, thus a slight bias towards severe cases may be present due to the sampling criteria.

Three subsets were generated for comparison with the complete data set (Appendix D): cases with shoulder impacts, cases with elbow impacts, and cases with head impact. In all subsets, cases were excluded if the group definition variables were unknown. To examine for which initial conditions shoulder or elbow impacts are likely to occur, some of the variables were chosen for further investigation. Vehicle speed, Maximum Abbreviated Injury Scale (MAIS) code and fatality were investigated as indicators of the accident severity. The direction from which the pedestrian was hit was examined in the context of elbow and shoulder impact. Finally head WAD, pedestrian size and the ratio of the two were investigated. In contrast to the FSR02 experiment, where head WAD was measured parallel to the vehicle centreline, head WAD was measured in GIDAS along the connection between the projection point on the ground below the leg-to-bumper contact point and the head impact point.

III. RESULTS

New experiment FSR02

The time stamps and WAD of the pelvis, elbow, shoulder and head impacts on the vehicle are shown in Table II, together with the depth of visible indentation on the vehicle caused by these impacts. Impact time was defined as first contact. No impact occurred on the right side of the vehicle. The longitudinal and lateral throwing distances were 11.2 m, and 1.8 m towards the left side of the vehicle, referred to the subject's CG.

TABLE II
IMPACT PARAMETERS IN FSR02

	Pelvis	Elbow	Shoulder	Head
Impact time [ms]	19	74	114	120
WAD [mm]	900	1640	1780	2000
WAD ratio (*)	1.10	1.43	1.24	1.23
Centre line offset [mm]	82	20	96	109
Vehicle part	BLE	Bonnet upper end	Windshield	Windshield
Crush depth [mm]	0	<10	0	85
(*) Reference height	Trochanter	Olecranon, initial height	Humeral head	Eye level

A visual inspection of the film captured by the posterior camera shows that the L4 target moved downwards 12 ms after the first contact, while the other targets remain stationary. T11 followed at approximately 15 ms, T2 and the head at 16 ms. When T2 started moving downwards, the scapula targets began to rotate upwards slightly in relation to the thorax. However, linear displacement of the scapula targets did not start until 26 ms after first contact. This indicates that it may not be gravity which induces the observed displacements of the head and spine in the first place, as gravity would cause the body to accelerate uniformly following support

release. The spine and head began moving before the pelvis contact (Table II). A hypothesis would thus be that the earliest spine and head movements are caused by energy propagation from the leg impact, with an amplifying effect from the pelvis impact shortly after. This hypothesis is supported by the observation that the spine seems to be drawn downwards in comparison to the surrounding tissue (Fig. C2 in Appendix C), leading to spine elongation. Still shots from four camera perspectives can be found in Fig. C1 in Appendix C.

2D linear displacements and 3D angular displacements obtained from the video analysis are shown in Fig. 2. Unfortunately, y-displacements were not considered trustworthy due to considerable distance between the camera and the subject. However, the centre line offsets in Table II give an indication of how the subject moved in the y-direction. The order of the rotations was: yaw in the original coordinate system, pitch in the rotated coordinate system, and finally roll in the latest coordinate system. Consequently, the angular position at each assessment point can be obtained directly from the graphs; however, comparison between the different body parts directly from the graphs is not possible. All link and interlink angles are shown in Fig. 4 and Fig. 5. Displacements in relation to the vehicle can be found in Fig. 3 and still pictures of the videos in different perspectives are given in Fig. C1 in Appendix C.

In the video, around the time of pelvis impact, a bi-axial lower torso rotation began, anticlockwise in the transverse plane (negative yaw), together with a slight rotation in the coronal plane (to the right, or negative pitch). Backward rotation in the sagittal plane (positive roll) appeared to start slightly later. Slight, but visible rotation of the vertebrae targets started at around 20 ms for L4, at 30 ms for T11 and at 38 ms for T2 (Fig. 2, Fig. C1 in Appendix C). Despite these initial vertebrae rotations, the thorax remained almost vertical until 60 ms after impact when it began rotating towards the vehicle (Fig. 3, Fig. 4). Following elbow contact, enhanced negative yaw made the subject's back turn towards the bonnet. Around the time of head impact the thorax pitch angle was estimated as -75°; the yaw angle as -50°.

The scapula began to rotate upwards after 16 ms, and started elevation and adduction while the thorax continued to fall. After the first elbow contact, close to the upper edge of the bonnet at 74 ms, the elbow continued the downward motion, causing it to slip over the edge and further down, where it impacted the windshield at 84 ms. During the contact phase, the elbow appeared to increasingly support the thorax in an anterolateral direction up to approximately 95 ms, enhancing the previous negative yaw rotation of the thorax and causing the right scapula to be elevated and to adduct. Furthermore, the elbow slipped forward and thus did not provide further support to the thorax, but caused the scapula to adduct before the shoulder impact. The shoulder was thus in a slightly elevated, anteriorly displaced position when it impacted the vehicle.

The head moved slightly differently than the vertebrae as visible rotation in the transverse plane started at around 40 ms. The head angular position in the transverse plane was negative (to the left) throughout the whole process. At around 16 ms, the time when the spine displacement began, the head started rotating in the sagittal plane and rolled slightly backwards. This movement was reversed shortly thereafter, resulting in a more distinct forward roll. Shortly after the elbow impact, the roll angular movement changed direction again, resulting in a positive (backward) roll angle at the time of head impact. Head rotation in the coronal plane started approximately at 55 ms and was directed to the left (positive pitch) at first. At around 82 ms, this movement was reversed, resulting in a fast rotation to the right (negative pitch, Fig. 2b).

This behaviour of the head, in combination with the thorax kinematics, determined the neck response. The neck slowly bent away from the vehicle until around 82 ms and then began bending rapidly towards the vehicle. From another perspective, it can be said that the neck sets the boundary conditions for the head motion. Thus, the neck behaviour, which determines the amount and location of coupling between the head and the thorax, can be considered important for detailed validation of the HBM head response.

Neck (head to T2) elongation could not be estimated as a function of time, since it was not possible to estimate the change of distance from the camera over time accurately. However, from the front-mounted video cameras and from the contact positions on the vehicle, i.e., the centre line offsets (Table II), the resultant head-to-T2 elongation could be estimated. Under the assumption of zero offset in y-direction, the minimum head to T2 elongation was calculated as 20 mm elongation at the time of elbow impact, 10 mm elongation at the time of shoulder impact and 12 mm compression at the time of head impact.
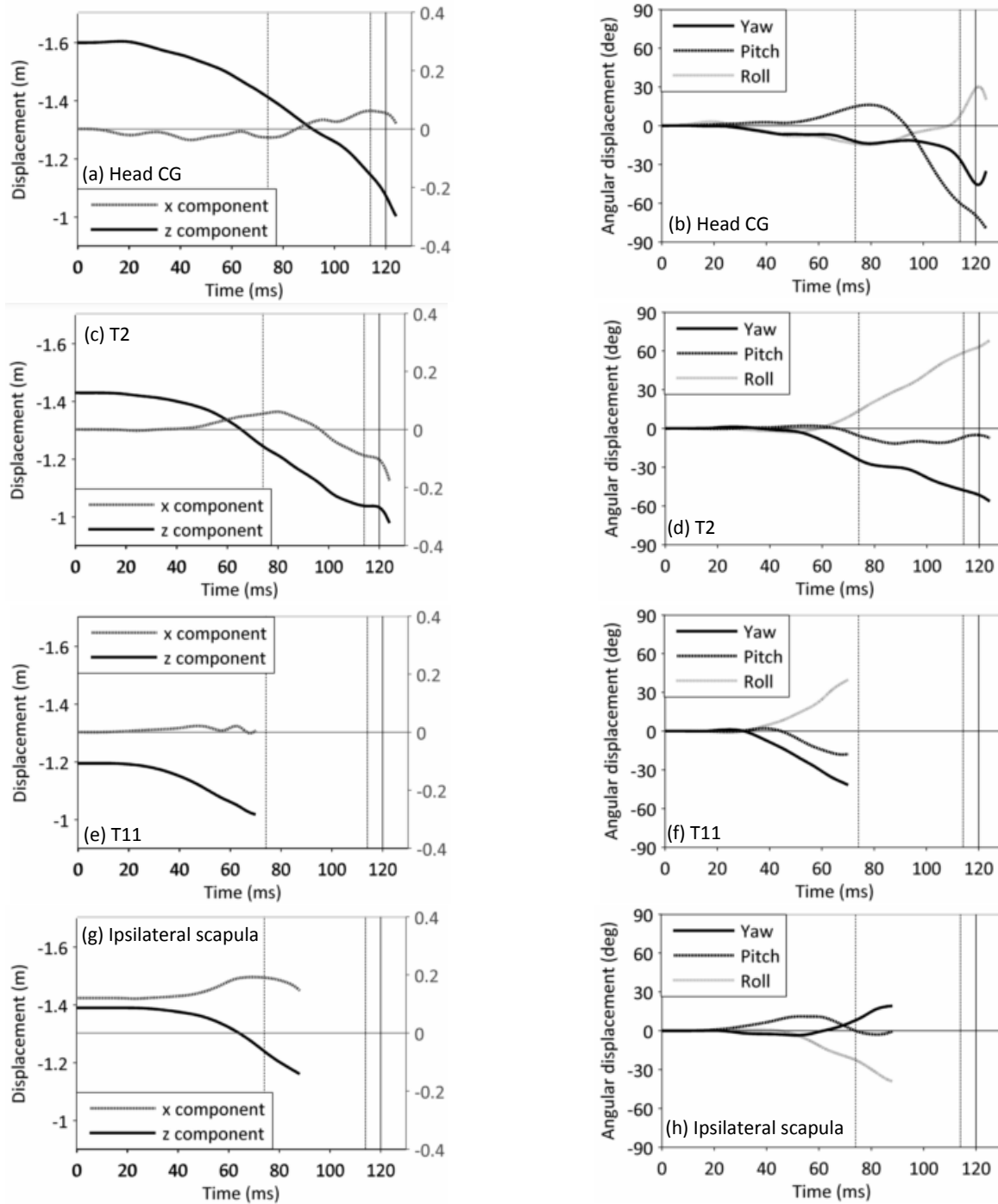
Fig. 2. Linear (left) and angular (right) displacements for head CG, T2, T11 and ipsilateral scapula in the FSR02 test, expressed in the global coordinate system (Fig. A1 in Appendix A).
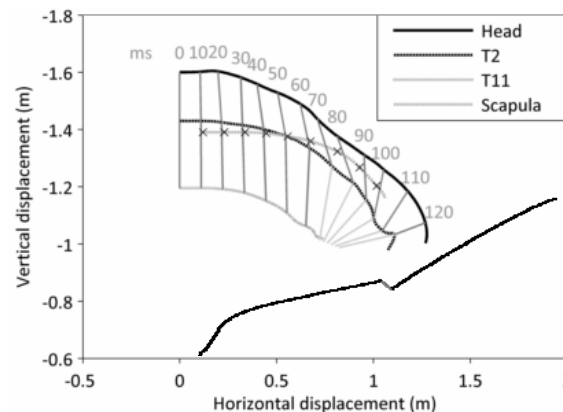

Fig. 3. Displacements of the head CG, T2 and T11 vertebral body centres and the scapulae in relation to the vehicle; test FSR02. Movement in y-direction was not considered. T11 displacement after 68 ms was estimated.
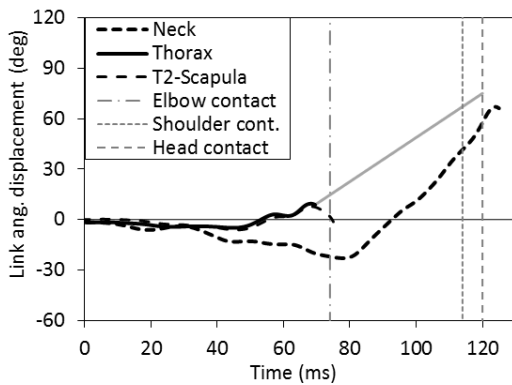
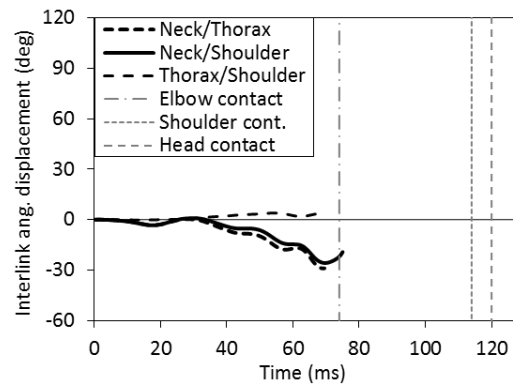Fig. 4. Link angular displacements, test FSR02. Thorax angle was estimated from 70 ms to head impact.

Fig. 5. Interlink angular displacements, test FSR02.

Reanalysis of H1, H2 and H3

The times of impact and locations of the pelvis, elbow, shoulder and head impacts on the vehicle in each test are shown in Table III. The impact time of each body part was defined as the first contact with the vehicle, determined from film analysis. Sketches from the tests can be found in Fig. B3, Appendix B.

Around the time of leg and pelvis impact, in comparison to the movement of the surrounding tissue, a downward motion of the spine was observed in the film, which is assumed to be a consequence of the initial leg or pelvis to vehicle contact. However, the spine relative to soft tissue motion was small, and hence difficult to assess. This was due to early release of the subjects and early start of their overall downward motion.

The thorax of the subjects' continuously rotated towards the vehicle in the coronal plane until head contact (Fig. 6b). Thereafter, the angle increased only slightly. Thorax rotation in the subjects' sagittal plane was not visible in any of the tests. After head impact and in the transverse plane, the thorax showed a slight clockwise rotation towards the vehicle in H1 and H3, whilst the contrary showed in the H2 test. The latter appeared to be the consequence of early leg and pelvis anticlockwise rotation.

After pelvis contact, the spine curved towards the vehicle (Thorax-Lumbar interlink angle, Fig. 7b). In H1 and H3, the curvature gradually ceased and the spine was straight close to the time of elbow impact. After head impact, spine curvature varied from test to test.

Thorax motion highly influenced neck and head kinematics. Due to the flexibility of the neck, head rotation was different to thorax rotation (Fig. 6a). In the sagittal plane and around the time of pelvis impact, the head began a slight forward rotation in the H1 and H2 tests, but then rotated rearward again such that the neck was neutral in the sagittal plane at the time of head contact. In the transverse plane, all head rotations began around the time of pelvis impact, directing the face away from the vehicle, and continued until elbow impact. In the coronal plane, while the thorax rotated towards the vehicle, the head lagged behind resulting in a lateral neck flexion. Around the time of elbow contact, the head began to rotate in a transverse and coronal direction towards the vehicle. This may be a result of the support that the elbow-shoulder complex provided for the thorax. However, in the H1 test, the upper arms were tied to the thorax. Thus, the elbow did not move away from the body as much as in the H2 and H3 tests, and for this reason provided less support for the thorax.

TABLE III
IMPACT PARAMETERS IN H1, H2 AND H3

		Pelvis	Elbow	Shoulder	Head
H1	*Impact time [ms]*	35	117	150	161
	Vehicle part	BLE	Bonnet	Bonnet	Bonnet / Windshield
H2	*Impact time [ms]*	38	104	134	142
	Vehicle part	Bonnet	Windshield	Windshield	Windshield
H3	*Impact time [ms]*	25	111	129	148
	Vehicle part	BLE	Windshield	Windshield	Windshield

Transverse head rotational velocity was low before impact and increased significantly during impact in the H1 test, in which the lower parietal bone hit the upper end of the bonnet and the upper parietal bone hit the windshield. In this case, the windshield appeared to have remained undamaged. In contrast, in the H2 and H3

tests, the arm moved freely and the elbow hit the lower region of the windshield in both tests. In the H2 test, the elbow cracked the windshield in the lower-left region but the rest of the windshield appeared to be intact before the head impacted. In the H3 test, the windshield appeared to suffer more damage due to the elbow and head impacting the previously cracked windshield. Head rotational velocity in the transverse plane just before impact was low according to video analysis and only minimal changes could be observed. The head seemed to be turned slightly towards the vehicle when hitting the windshield.
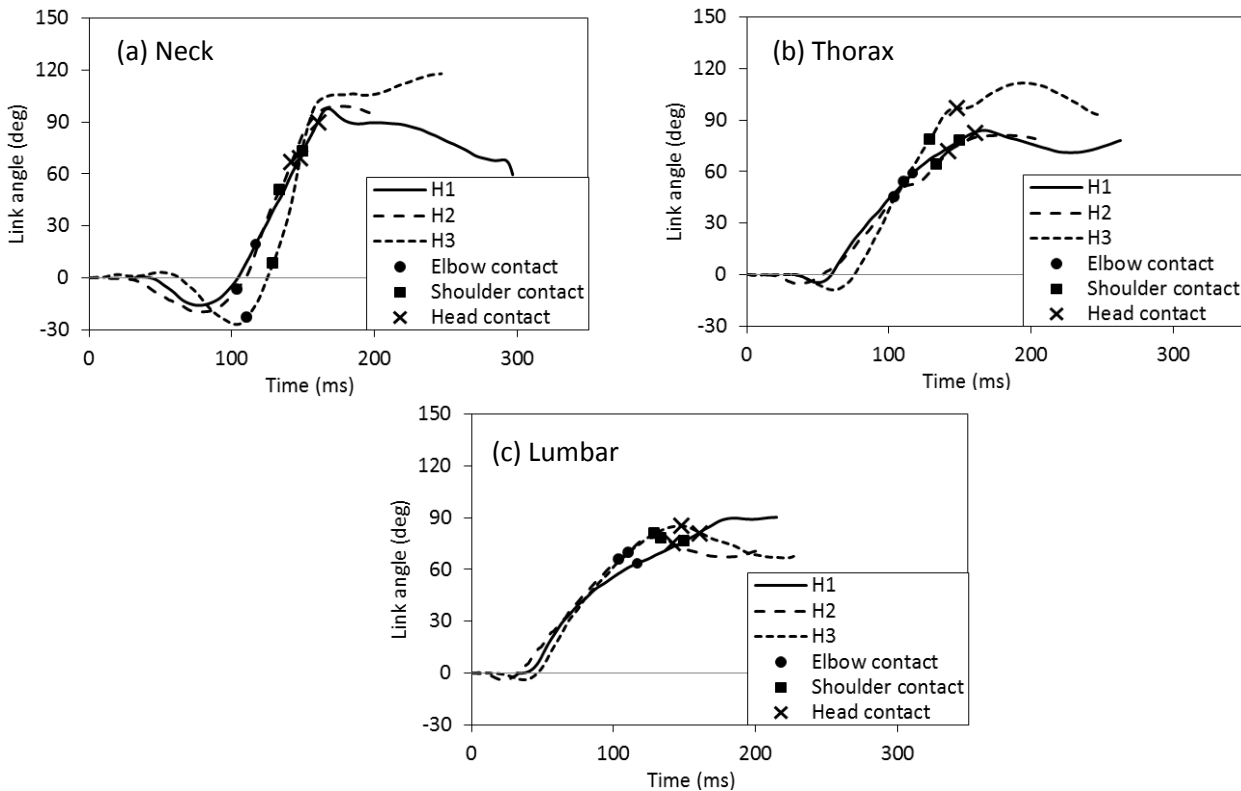
Fig. 6. Link angular displacements projected into the film plane; tests H1, H2 and H3.
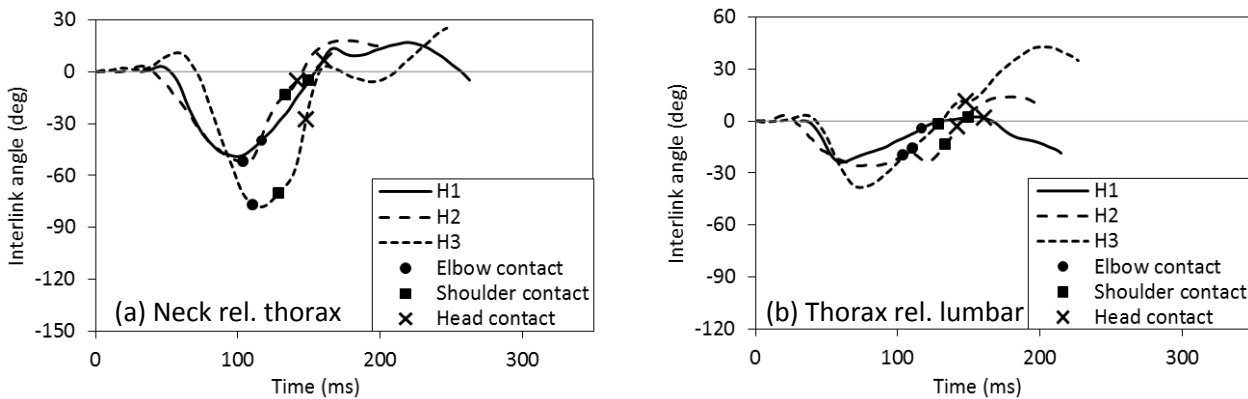
Fig. 7. Neck relative to thorax (a) and thorax relative to lumbar (b) angular displacements; tests H1, H2 and H3.

As the shoulder and elbow movement was restricted in the H1 test, the upper arm motion in this test was considerably different from the other tests. Therefore, this motion will not be described in further detail. In the H2 and H3 tests, while the thorax continued to fall onto the bonnet, the humerus was abducted, probably due to gravitational effects. Following elbow impact, the humerus-scapula complex was elevated and the scapula seemed to be adducted when the shoulder impacted the vehicle.

Displacements, both in relation to the vehicle and to the laboratory coordinate system, can be found in Appendix B, Fig. B1 – Fig. B4. Sketches including photo target locations can be found in Appendix B, Fig. B5.

Accident data

The GIDAS search returned 1,212 pedestrians listed in Table D-I in Appendix D. In 90 % of the cases, the pedestrians were reported to be hit laterally or almost laterally. In 17 % of all cases, a shoulder impact was reported to occur, while elbow impact was reported in 9 % of the cases. Looking at the 164 MAIS 3-6 cases,

shoulder and elbow impacts were reported in 26 % and 12 % of the cases respectively. Similar numbers were found for fatal cases. In cases where a head impact had occurred, shoulder and elbow impacts were found in 29 % and 10 % of the cases respectively. Whether pedestrians impacted with their shoulder or elbow seemed to be independent of impact directions. Vehicle impact speeds, pedestrian size, head WAD and head WAD to size ratio did not differ significantly between the different subgroups, even though vehicle impact speeds tended to be higher in both the shoulder and the head impact subgroup, compared to all cases. Removing children from the sample did not change the investigated parameters significantly; thus, they were included in the statistics.

IV. Discussion

Limitations

It is unknown to which extent the subject conservation method in test FSR02 may have influenced the results. Even though PMHSs lack active musculature, they are the most accurate available surrogate for humans in pedestrian testing. Furthermore, as this study investigated the kinematics of the subject and not the sustained injuries, it is expected that the difference to a fresh cadaver is relatively small, especially when taking into account the level of violence involved during an accident. For the H1, H2 and H3 tests, the subject conservation method is unknown.

In the FSR02 test, some targets were not clearly visible during the whole impact, mainly due to rotation away from the camera. Only reliable results were deemed appropriate to include in this study, therefore, some graphs appear to be incomplete. Similarly, the substantial camera distance affected the displacement measurement in the out-of-plane component; therefore, the y-displacements are not shown for the FSR02 test. The rotational component around the y and the z-axis were judged as acceptable in terms of reliability and all other displacement components were of high accuracy. The latter was a result of the substantial camera distance. Errors were estimated to be less than 5 mm in linear and 5° in rotational displacements.

In the H1, H2 and H3 tests, scaling of film data was an issue due to a lack of applicable reference film targets. Multiple methods were applied to scale the film data. Using the distance between the spine targets resulted in displacements as in [16] and was thus considered the most appropriate method, despite having only been measured when the PMHSs were lying down. Kerrigan et al. suggested [7] that the PMHSs may have a different distance (up to 8 %) between spine targets when in test position, compared to when lying down. Thus, using the photo targets on the spine for scaling can result in considerable errors. The scaling procedure used in [16] is unknown. However, such change in distances was not observed in FSR02.

Comparison with other full-scale tests

The PMHS's kinematics observed in this study resembled those in other full-scale pedestrian studies in which the subject was impacted laterally. Four previous studies were selected for comparison with the results in this article: Kerrigan et al. [7] studied the response of three PMHSs when impacted by a small sedan at 40 km/h; similarly, Kerrigan et al. [8] exposed two subjects to a 40 km/h collision with a SUV; in Kerrigan et al. [9] seven PMHS were used to study the influence of anthropometry on response to 40 km/h impacts by a mid-size sedan; and finally in Subit et al. [21], four PMHSs were used to study the response when impacted by a mid-size sedan or a small city car traveling at 40 km/h. Despite the body kinematics in the four studies were presented slightly differently, it was possible to perform qualitative comparisons of the studies.

Following pelvis-to-vehicle contact, the spine of the subjects moved somewhat downward and the lumbar and thoracic spine flexed laterally away from the vehicles in this study. This correlated well with the results of the other studies [7]-[9], [21]. Similar amount of spine flexion was observed for the two mid-sized PMHSs when impacted by mid-size sedans. However, while subject H1, H2 and H3 in this study exhibited lateral flexion motion at a range of 25 to 39 degrees (Fig. 7), only one of three subjects exhibited lateral flexion motion to the same degree when hit by a small sedan [7] and only one out of two PMHS when hit by a SUV [8]. Remarkably, none of the four subjects exposed to a mid-size sedan or a small city car [21] exhibited similar amount of spine lateral flexion. These similarities and differences are difficult to explain; possibly the difference is due to variations in front geometry between the vehicles used, and variation differences of a biological nature.

The head lagged behind the T1 (neck flexion away from the vehicle) in most of the full scale pedestrian tests in the studies used for comparison, as well as in this study. Taking all studies into account, the amount of lagging appeared to be independent of vehicle model. However, the amount of head lag appeared to be inverse to the

amount of combined lumbar and thoracic spine flexion in the studies used for comparison, with an exception for subject C3 [21]. Nevertheless, simultaneous lateral flexion for the lumbar and thoracic spine, as well as, for the neck for subject H1, H2 and H3 was noted in this study. In these tests the neck link relative to the thorax link reached an average lateral extension of 60 degrees (Fig. 7). Such large lateral neck extension was only seen in three out of eleven subjects in the studies used for comparison. In half of the subjects in this and compared studies, the head lag peaked and was reduced before the elbow or shoulder made vehicle contact.

For six of the eleven subjects in the comparison group, the head still lagged or the neck was just aligned with the thorax spine at head contact. Similar variations could be observed in this study; subject H3 still exhibited neck relative to thorax flexion away from the vehicle while for subject H1 and H2 thorax flexion was minimal.

Substantial humerus adduction occurred in three out of four tests in this study. In the FSR02 test, the humerus was virtually vertical when the elbow contact permanently deformed the rear bonnet trailing edge. Similar humerus motion was observed in the H2 and H3 tests; however, in these tests the elbow broke the windshield, it was severely damaged in H3, and subsequently making contact with structures behind the windshield and the elbow appeared to be immobilised. Elbow contacts also occurred in studies used for comparisons. However, as a result of tying together the subject's hands together, it appears that the humerus was pointing forward at an oblique angle. As a result the elbow hit the vehicle forward of the thorax and later than in this study. Due to the types of elbow contact that occurred in this study, the thorax and head kinematics after elbow contact were to some degree different to those previously reported. However, in this test, the load transferred through the humerus did not slow down the motion of the thorax towards the bonnet and windscreen. In this test the load made the thorax rotate around its local z-axis (in yaw). One contributing factor may have been the position of the struck side limb; in the FSR02 test the struck limb was in front of the other whereas in all other tests discussed herein, the struck side limb was rear of the other. As a consequence of the thorax rotation, the shoulder complex made vehicle contact with the lowest region of the windshield just before the head. Hence, in the FSR02 test the shoulder complex had limited influence on the head rotational velocity and on reducing head relative to vehicle velocity. In the H2 test, the loads transferred through the humerus clearly reduced the thorax velocity towards the vehicle. Consequently, the head rotational velocity towards the vehicle appeared to increase considerably. In test H3, the loads through the humerus appeared to have less influence on the thorax motion and the subsequent shoulder impact had a more pronounced effect on head kinematics.

In the comparison studies the shoulder also made vehicle contact before head contact occurred. An effect of such shoulder contact is a reduction of the thorax relative to vehicle velocity but due to these changed boundary conditions the head relative vehicle velocity may be increased as the neck flexes towards the vehicle. In one study the average resultant head relative to vehicle velocity was approximately 10 % higher than the initial vehicle speed [7]. However, in the study in which SUVs were used, the resultant velocity was reduced to about 75 % of the initial vehicle velocity [8]. In the H2 and H3 tests, these velocities were at least 30 % higher than initial vehicle velocity.

In summary, pelvis to vehicle interaction leads to lumbar and thoracic spine extension that appeared to vary depending on the vehicle front and variation of a biological nature. The fourth mentioned extension appears to influence the amount of head relative to thorax lag. Large lag of this type may result in high head rotational velocity at the time of head contact with vehicle. Tying the subjects´ hands before the test influences elbow to vehicle contact and this appeared to influence thorax and head kinematics. The conclusion is that in order to validate HBMs, additional test series should be performed using a large number of subjects to compensate for variability, and using modern vehicles. The humerus and the scapula kinematics should be studied further since they appear to influence the thorax response. Additionally, complementary test series should be conducted where the hands of the PMHSs are not tied together.

Comparison with shoulder impactor tests

Several shoulder impactor tests have been conducted in the past, some of these used PMHSs [22] and others were performed with volunteers [23]. For the PMHS tests, the severity varied from non-injurious to injurious, and impact angles were also varied. However, for all tests, the locations of the impacts were close to the head of the humerus, and the impact was perpendicular to the vertical axis of the PMHS or volunteer when seated. An additional limitation was that the scapula was adjusted to a neutral position. Consequently, none of the tests were performed with the scapula in adducted or elevated position. Our full scale PMHS results indicate that the shoulder in a pedestrian accident will be loaded differently. Therefore, it would be beneficial to design and

perform additional impactor tests in which the loading conditions are tailored to represent the pedestrian kinematics observed in this and other full scale pedestrian collision studies. Furthermore, since the results in this study suggests that elbow and shoulder contact may influence thorax kinematics, as well as head rotation just before head impact, further study of the shoulder and thorax kinematics due to elbow loads transmitted through the humerus should be aimed at. Here, a numerical study using a validated HBM can help in understanding the importance of the elbow-car interaction for head injury prediction.

Comparison of PMHS full scale test data with accident data

Validation data should be representative of the accidents that occur in real life. The experiments presented in this study are typical of a few of the sampled real life accident cases. The selected vehicle speed used, the impact direction relative to the PMHS, and the resulting WAD, were representative of the unweighted accident data sample. However, for these variables there was a considerable variation in the accident data. Hence, the necessity to perform additional PMHS full-scale tests using different set-ups to enable validation of HBMs for all types of pedestrian accidents that occur in real life, is evident.

It is interesting to note that many cases do not report shoulder and elbow impacts. A comparison of the frequency of elbow and shoulder impacts in lateral pedestrian PMHS tests could not be found in literature. Both shoulder and elbow impacts occurred in the PMHS tests in this study, which does not correlate with the accident data. Elbow and shoulder impacts were reported in only 17 % and 9 % cases respectively, of all accidents sampled for this study. However, for AIS3+ these fractions were slightly larger: 26 % and 11 %, respectively, which may possibly be due to avoidance reactions of the pedestrian. This indicates that influence of muscle strength and muscle activation may play a role in pedestrian impact kinematics and injury outcome. PMHS tests provide the most biofidelic data to evaluate HBMs and mechanical models; however, additional data may have to be considered when developing detailed pedestrian models. Furthermore the impact speeds in a fair amount of the accidents were low and consequently, considering a possible avoidance reaction, upper body contact may not have taken place – in 62% of the accident cases, there was no head impact reported. However, in the FSR02 test, paint markings on the vehicle were the only indication that a shoulder impact occurred, which implies that shoulder impact may be difficult to detect in a real life accident. Despite these ambiguities, the difference between PMHSs kinematics and real life data supports the conclusion that shoulder and elbow impacts in pedestrian accidents, muscle tensioning before impact, and its effect on the thorax and head kinematics during a pedestrian accident, should be further investigated.

V. Conclusions

This study provides new pedestrian kinematics data for future model validation. 2D translations and 3D rotations were measured in a new full-scale pedestrian test focusing on spine, head and scapula kinematics. Re-analysis of three full-scale pedestrian tests provided additional information on shoulder kinematics and spine curvature over time.

Visual inspection of the films showed that the spine is drawn caudally in relation to the surrounding soft tissue soon after first impact, inducing rotation of the head. In the new test, this motion actually begins before pelvis impact. The mechanism was observed in all four tests, involving two different vehicle geometries and four different subject anthropometries.

Head rotation deviates from thorax rotation in all rotational components, indicating that both the cervical spine properties and the location of the head centre of gravity in relation to the atlantoaxial joint play an important role with regards to quantification of head rotation before head impact. Elbow and shoulder impact seem to influence head rotation and it is assumed that they provide additional support for the thorax and thus change neck boundary conditions such that the head displays rotational acceleration towards the vehicle.

In comparison with real life accident data, the test set-up appeared to represent the unweighted accident data sample in terms of impact velocity and head WAD. However, shoulder and elbow impacts were more likely to have occurred in cases with AIS3+ injury outcomes in relation to the complete sample. This suggests that shoulder and elbow impact are linked to severe injuries.

The results necessitate further investigation of shoulder impacts with the scapula elevated and adducted, and an abducted humerus. Similarly, elbow impacts with an abducted humerus should be studied for information on how energy is transferred from the elbow through the humerus and shoulder to the thorax.

VI. ACKNOWLEDGEMENT

VII. REFERENCES

[1]   WHO Regional Office for Europe, "European status report on road safety: towards safer roads and healthier transport choices. Copenhagen, 2009" Internet: http://www.euro.who.int/__data/assets/pdf_file/0015/43314/E92789.pdf, 2011-09-21 [2012-03-30]

[2]   Odero W, Garner P, Zwi A, Road traffic injuries in developing countries: a comprehensive review of epidemiological studies, *Tropical Medicine and International Health*, Vol. 2, No. 5, pp. 445–460, 1997

[3]   Hedlund J, "Pedestrian Traffic Fatalities by State – 2012 preliminary data" Internet: http://www.ghsa.org/html/publications/pdf/spotlights/spotlight_ped.pdf, 2011-01-19 [2012-03-30]

[4]   Alan M. Voorhees, "2011 Pedestrian Safety Tracking Report" Internet: http://njwalksandbikes.files.wordpress.com/2011/11/2011-pedestrian-safety-tracking-report-final.pdf, 2011-10-05 [2012-03-30]

[5]   Organization for Economic Cooperation and Development (OECD), "Safety of Vulnerable Road Users", DSTI/DOT/RTR/RS7(98)1/FINAL. Paris: OECD, Directorate for Science, Technology, and Industry, Scientific Expert Group and the Safety of Vulnerable Road Users, 1998.

[6]   Chang D, "National Pedestrian Crash Report" Internet: http://www-nrd.nhtsa.dot.gov/Pubs/810968.pdf, 2008-07-10 [2012-03-30]

[7]   Kerrigan J R, Murphy D B, Drinkwater D C, Kam C Y, Bose D, Crandall J R, Kinematic Corridors for PMHS Tested in Full-Scale Pedestrian Impact Tests, *Proceedings of the 19th ESV Conference*, Washington D.C., Paper No. 05-0395, 2005.

[8]   Kerrigan J R et al., Kinematic Comparison of the Polar-II and PMHS in Pedestrian Impact Tests with a Sport-Utility Vehicle, *Proceedings of IRCOBI Conference*, Prague, pp. 159-174, 2005

[9]   Kerrigan J R, Crandall J R, Deng B, Pedestrian Kinematic Response to Mid-Sized Vehicle Impact, *Int. J. Vehicle Safety*, Vol. 2, No. 3, pp. 221-240, 2007

[10] Masson C, Serre T, Cesari D, Pedestrian-Vehicle Accident: Analysis of 4 Full Scale Tests with PMHS, *Proceedings of the 20th ESV Conference*, Lyon, Paper No. 07-0428, 2007

[11] Thollon L et al., How to Decrease Pedestrian Injuries: Conceptual Evolutions Starting From 137 Crash Tests, *The J. of Trauma, Injury, Infection, and Critical Care*, Vol. 62(2), pp. 512-519, 2007

[12] Chandalon S et al., A Comparative Study Between Subsystem and Global Approaches for the Pedestrian Impact, *Proceedings of the 20th ESV Conference*, Lyon, Paper No. 07-0429, 2007

[13] Kerrigan J R, Crandall J R, Deng B, A Comparative Analysis of the Pedestrian Injury Risk Predicted by Mechanical Impactors and Post Mortem Human Surrogates, *Stapp Car Crash J.*, Vol. 52, 2008

[14] Kerrigan J R, Arregui C, Crandall J R, Pedestrian Head Impact Dynamics: Comparison of Dummy and PMHS in Small Sedan and Large SUV Impacts, *Proceedings of the 21st ESV Conference*, Stuttgart, Paper No. 09-0127, 2009

[15] Elliott J R, Simms C K, Wood D P, Pedestrian Head Translation, Rotation and Impact Velocity: The Influence of Vehicle Speed, Pedestrian Speed and Pedestrian Gait, *Accident Analysis and Prevention*, Vol. 45, pp. 342-353, 2012

[16] Schroeder G, Konosu A, Ishikawa H, Kajzer J, Verletzungsmechanismen des Fußgängers bei Kollisionen mit einer modernen Fahrzeugfront – eine experimentelle Studie, *Kongressbericht 1999 der Deutschen Gesellschaft für Verkehrsmedizin e.V.,* Berichte der Bundesanstalt für Straßenwesen (BASt), *Mensch und Sicherheit*, Vol. 111, 1999.

[17] WHO Regional Office for South-East Asia, "Regional Report on Status of Road Safety: The South-East Asia Region" Internet: http://whqlibdoc.who.int/searo/2009/9789290223559_eng.pdf, 2009-11-18 [2012-03-30]

[18] Winkler G, Manuel d'Anatomie Topographique et Fonctionnelle, 2nd ed. *Masson*, Paris, 1974.

[19] EEVC-Working Group 17, "Improved test methods to evaluate pedestrian protection afforded by passenger cars" Internet: http://www.unece.org/fileadmin/DAM/trans/doc/2006/wp29grsp/ps-187r1e.pdf, Sept. 2002 [2012-03-30]

[20] Otte, D., Krettek, C., Brunner, H., Zwipp, H., Scientific approach and methodology of a new in-depth investigation study in Germany so called GIDAS, *Proceedings of the 18th ESV Conference*, Nagoya, Paper No. 161., 2003

[21] Subit D et al., Pedestrian-Vehicle Interaction: Kinematics and Injury Analysis of Four Full-Scale Tests, *Proceedings of IRCOBI Conference*, Bern, pp. 275-294, 2008

[22] Koh S-W et al., Shoulder Injury and Response Due to Lateral Glenohumeral Joint Impact: An Analysis of Combined Data, Stapp Car Crash J., Vol. 49, pp 291-322, 2005

[23] Ono K et al., Biomechanical Responses of Head/Neck/Torso to Lateral Impact Loading on Shoulders of Male and Female Volunteers, *Proceedings of IRCOBI Conference*, Prague, pp. 383-396, 2005

VIII. APPENDIX

Appendix A: Definition of coordinate systems and link angles

The coordinate system is defined such that the x-axis points from the subject towards the vehicle. In all graphs where x-coordinates are displayed, the vehicle moves from the right to the left. The y-axis points from the subject's anterior to its posterior. The z-axis is defined in the direction of gravitational force where zero is the ground and higher altitude is negative.

Roll, pitch and yaw are defined in analogy to aeronautical and automotive engineering terms, where a body "rolls" when it rotates around its x-axis, "pitches" when it rolls around its y-axis, and "yaws" when it rolls around its z-axis. With a right-hand definition of positive rotation, positive roll is a backward rotation in the sagittal plane. Positive pitch is a rotation in the coronal plane with the upper body away from the vehicle, and positive yaw is a rotation in the transverse plane where the anterior side turns towards the vehicle.
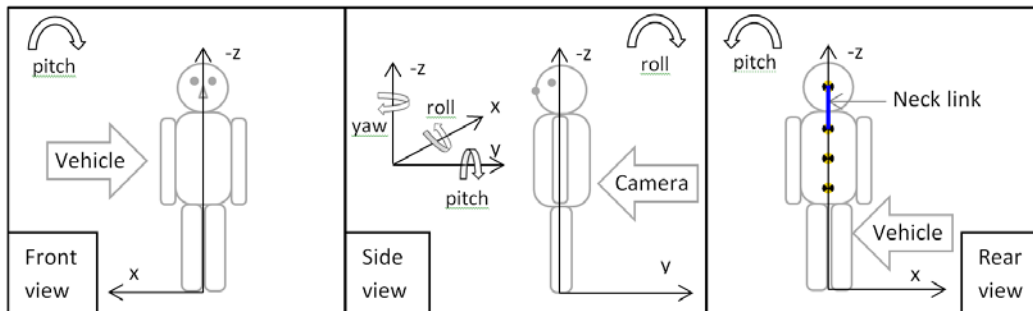
Fig. A2. Coordinate systems used in the analysis of both the new and previous PMHS test. The ipsilateral leg was positioned slightly in front of the CG in FSR02 and slightly behind the CG in H1-H3.

Appendix B: Further information on the H1, H2, H3 tests

In this section, the trajectories are scaled according to the previous publication [16].
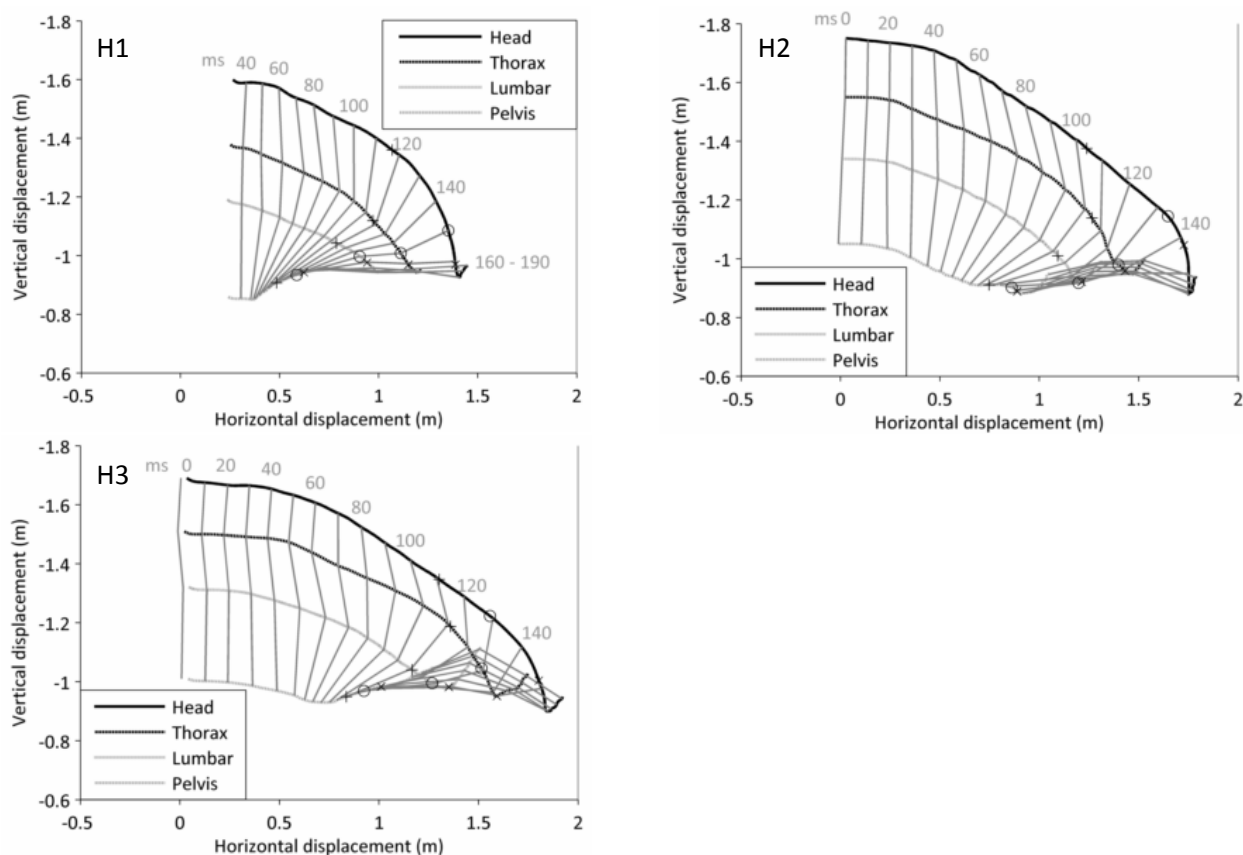
Fig. B1. Displacement relative to vehicle in test H1 (30 km/h), H2 and H3 (40 km/h). "+", "o" and "x" mark elbow, shoulder and head impact time, respectively.
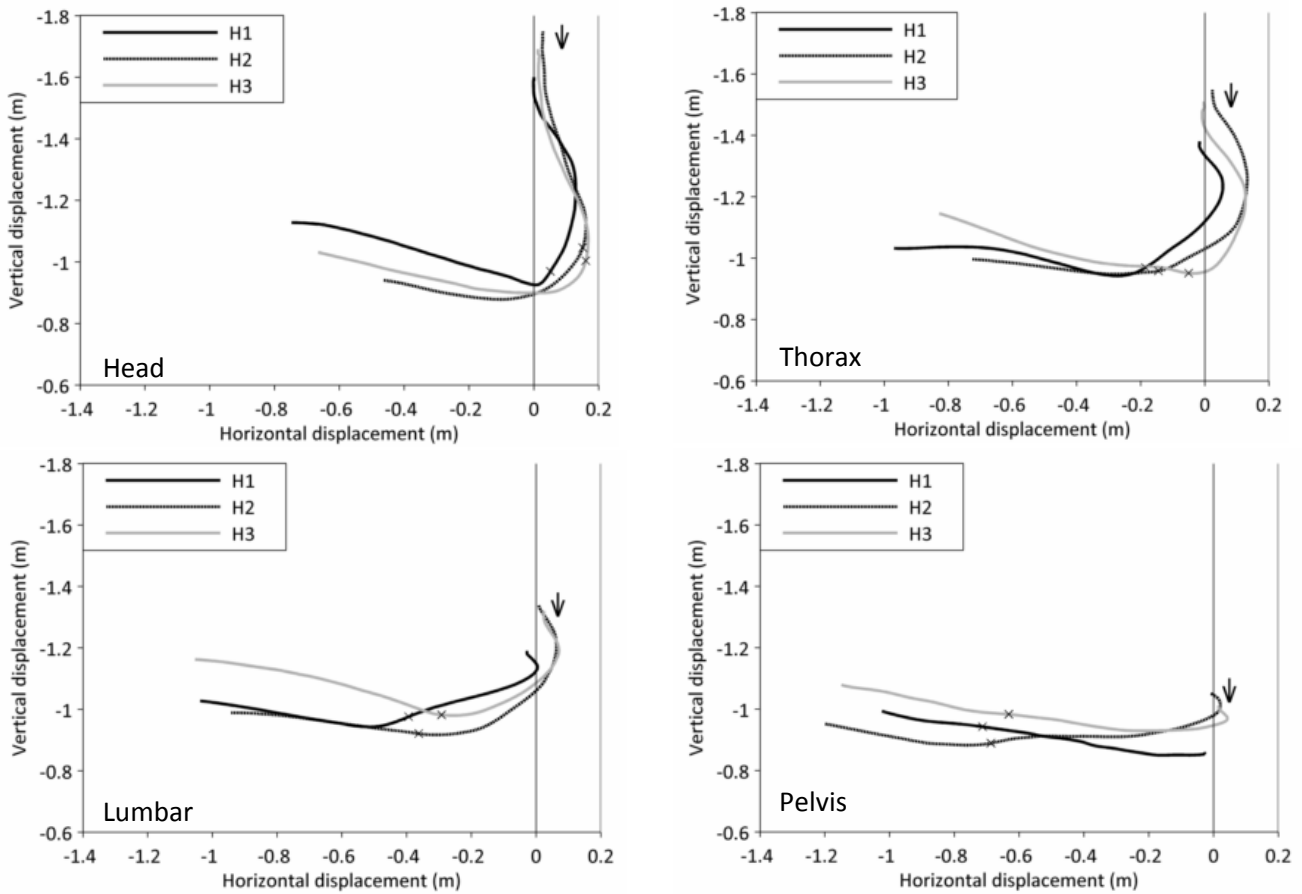
Fig. B2. Head, thorax, lumbar and pelvis trajectories in laboratory coordinate system, tests H1, H2, H3. Head impact is marked by "x" in each curve.
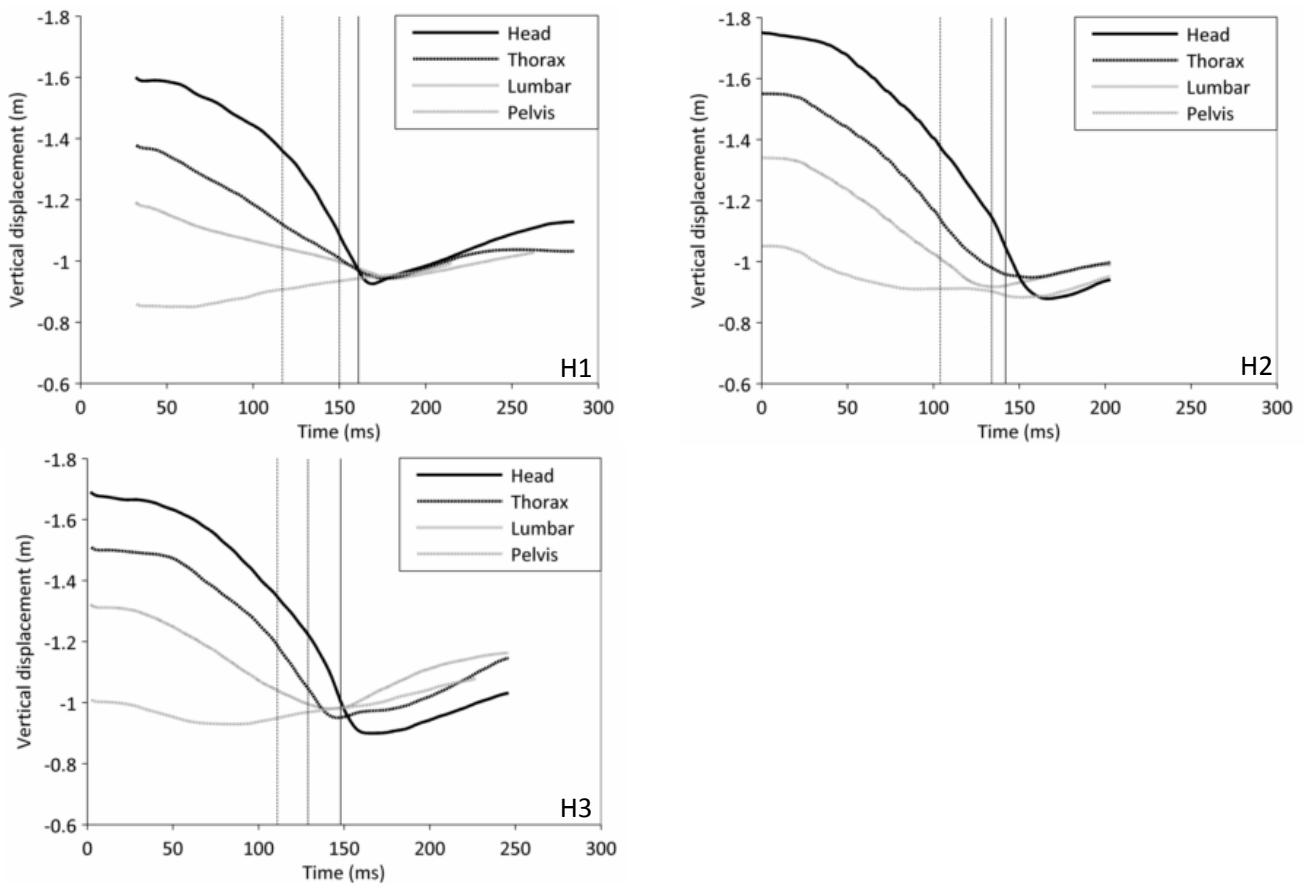
Fig. B3. Vertical displacement in test H1, H2, H3. Vertical grey lines mark elbow, shoulder and head impact.
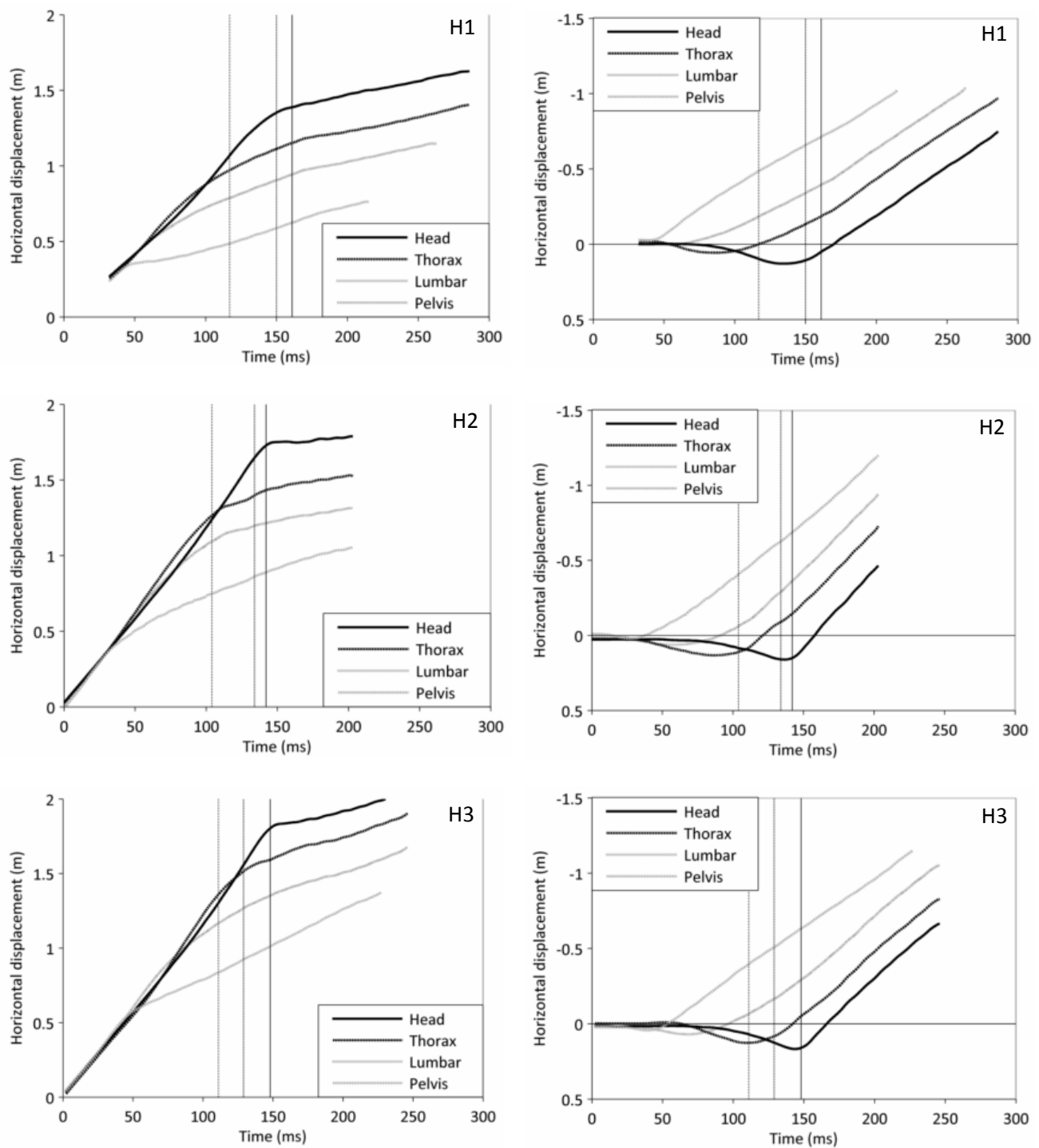
Fig. B4. Horizontal displacements in tests H1, H2, H3. Left side: displacement relative to vehicle, right side: displacement expressed in global coordinates. Vertical grey lines mark elbow, shoulder and head impact.

0 ms

20 ms

40 ms

60 ms

80 ms

100 ms

120 ms

140 ms

160 ms

180 ms

H1   H2   H3
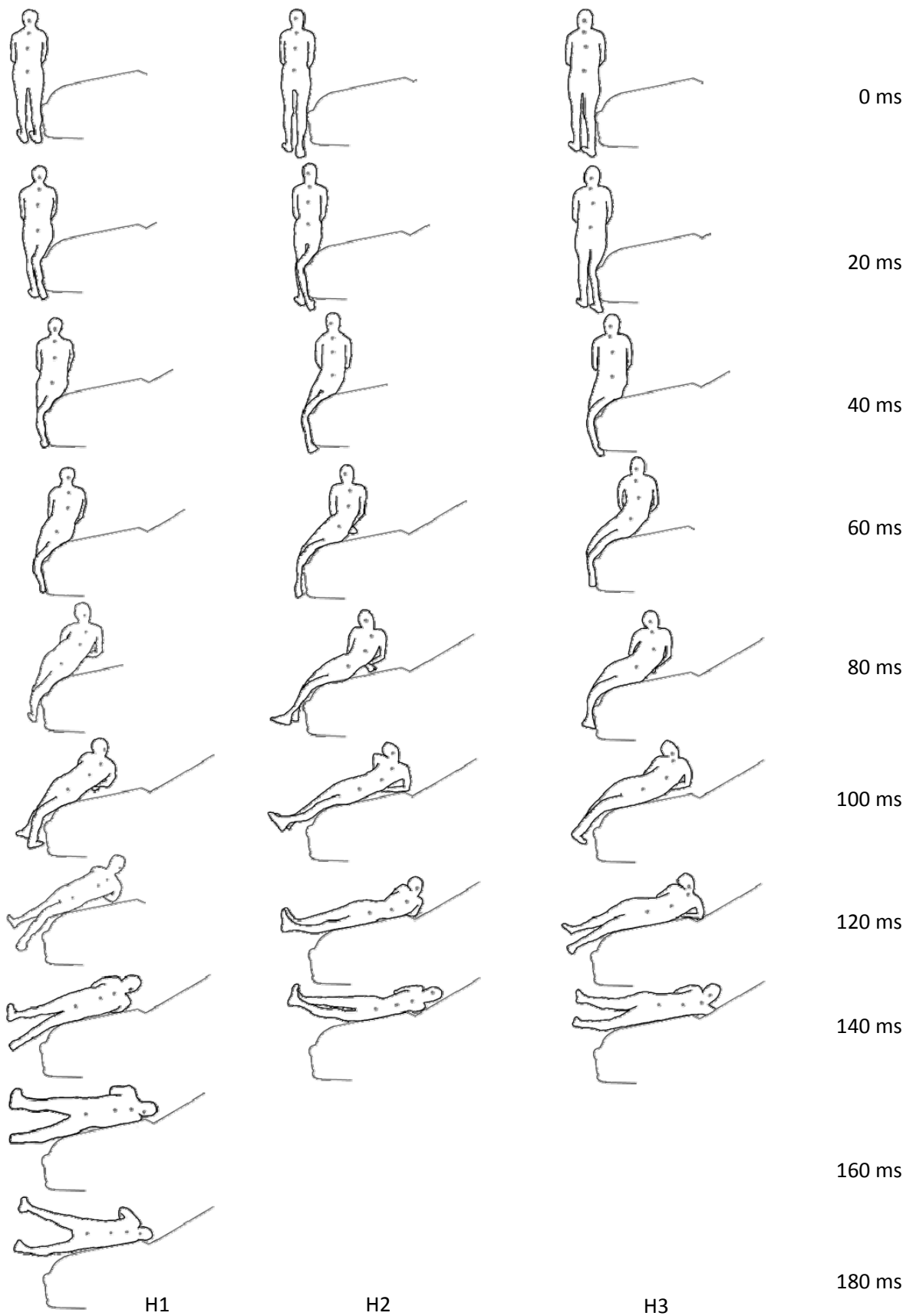
Fig. B5. Sketches of tests H1, H2 and H3. The dots indicate the locations of the photo targets (head, T1, T8 and sacrum), illustrating the spine curvature and the rotation of the head and thorax.

Appendix C: Pictures, test FSR02
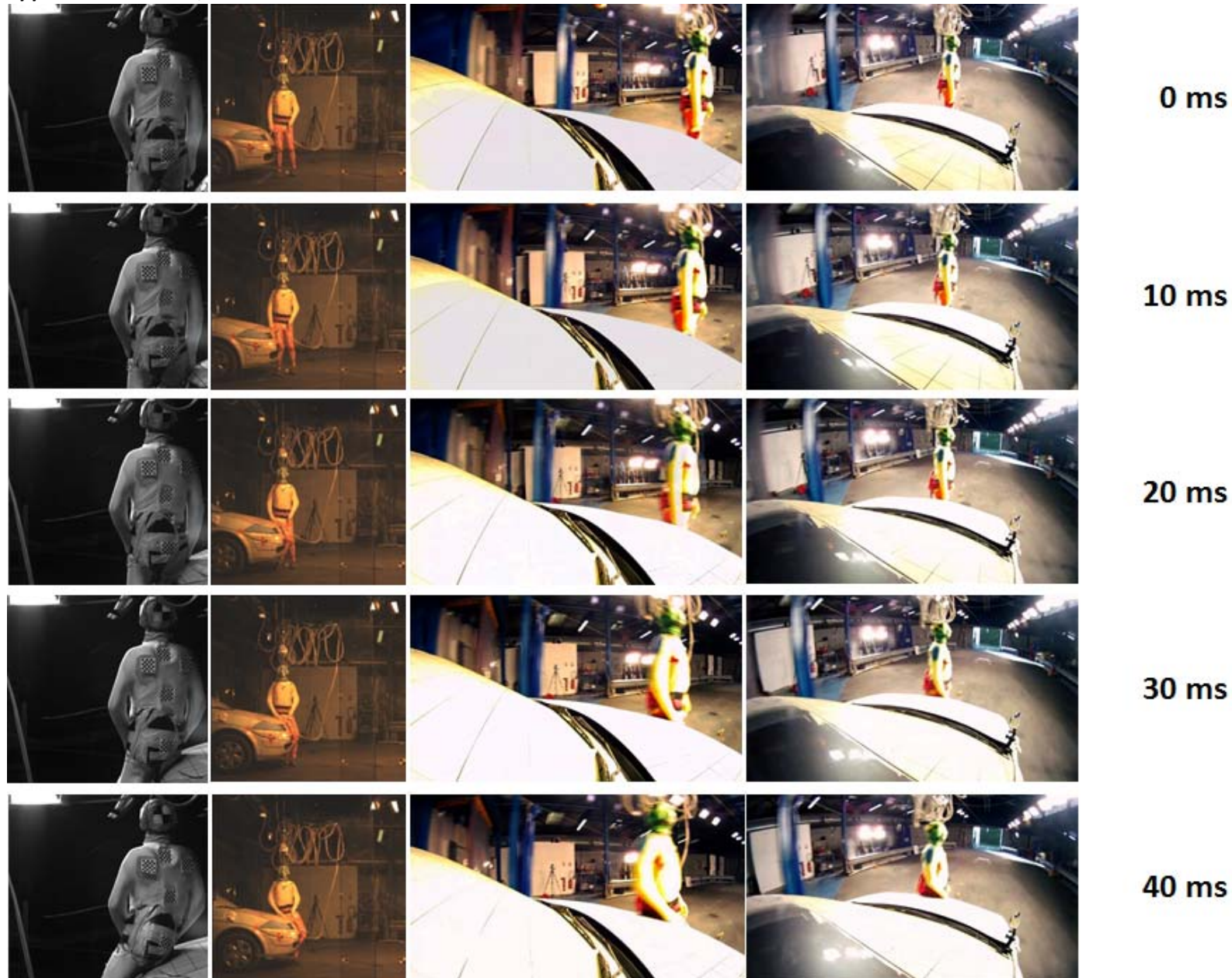
Fig. C1a: FSR02 in four camera views. From left to right: rear view, frontal view, on-board camera 1 and on-board camera 2.
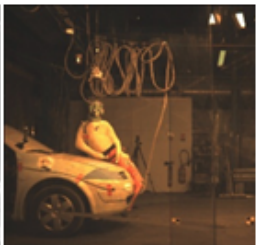
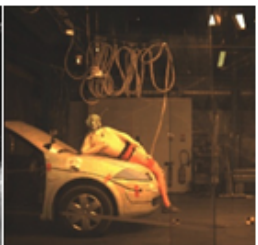|				
		No image available / image extremely blurred	No image available / image extremely blurred	50 ms
		No image available / image extremely blurred		60 ms
			No image available / image extremely blurred	70 ms
				80 ms
		No image available / image extremely blurred	No image available / image extremely blurred	90 ms

Fig. C2b: FSR02 in four camera views. From left to right: rear view, frontal view, on-board camera 1 and on-board camera 2.
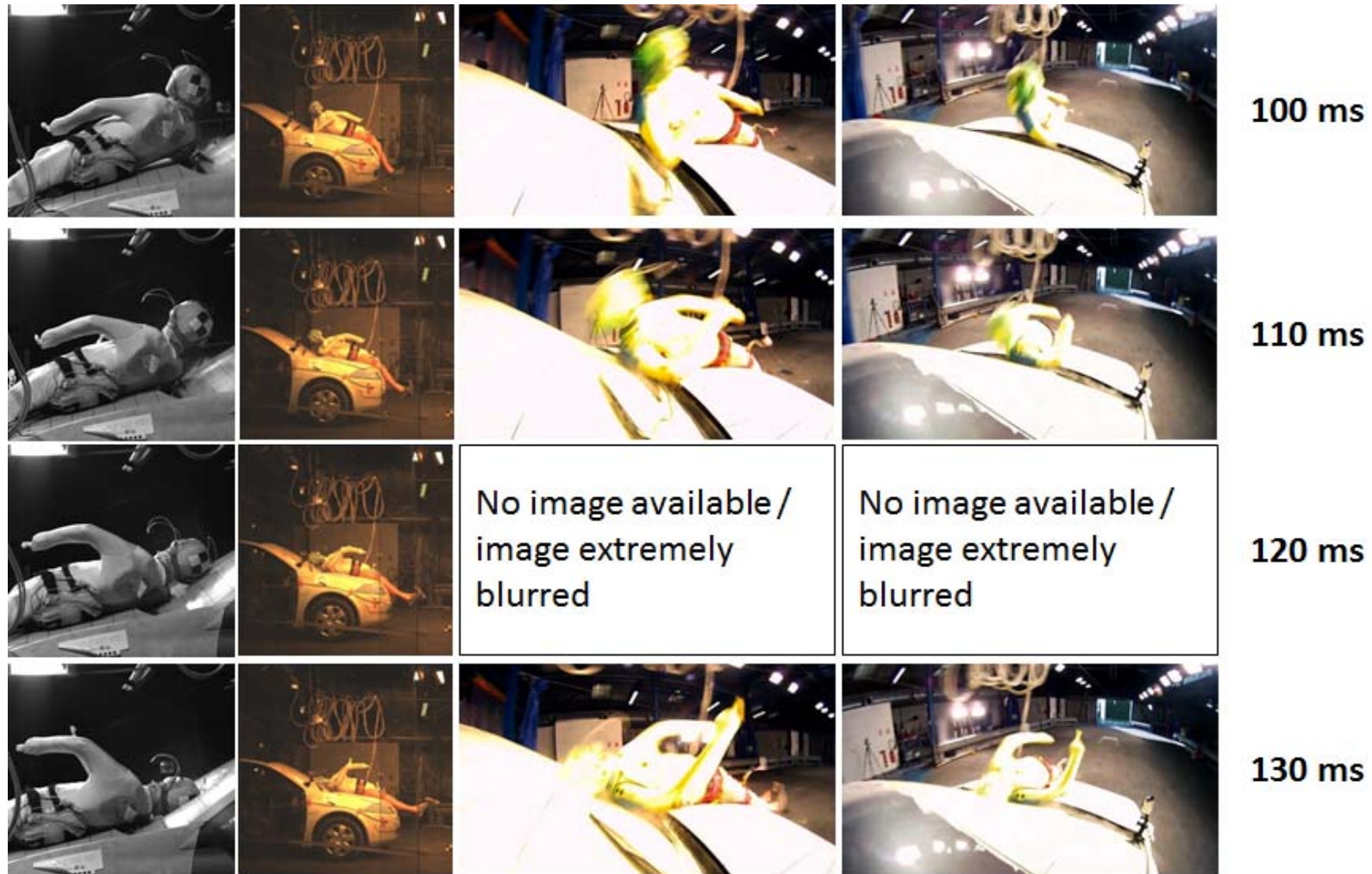
Fig. C2c: FSR02 in four camera views. From left to right: rear view, frontal view, on-board camera 1 and on-board camera 2.
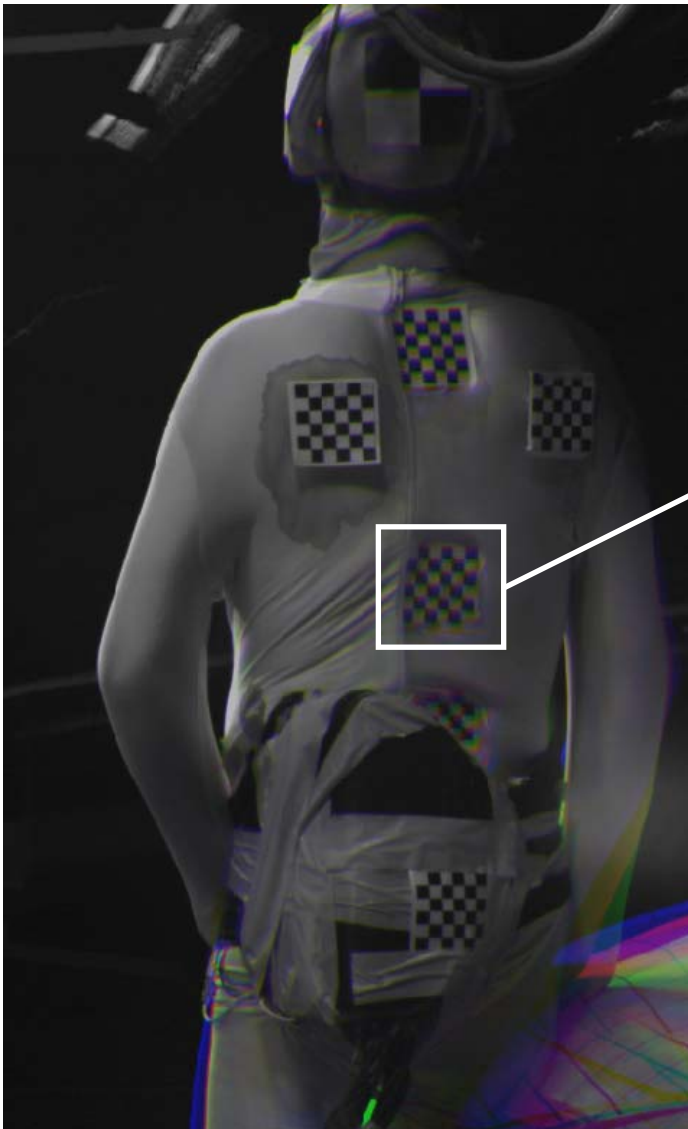
Fig. C2a: Coloured overlap of the times 10, 15, 20 and 25 ms in test FSR02. The spine targets are coloured, indicating spine motion, while the rest of the upper body is grey and thus does not show motion.
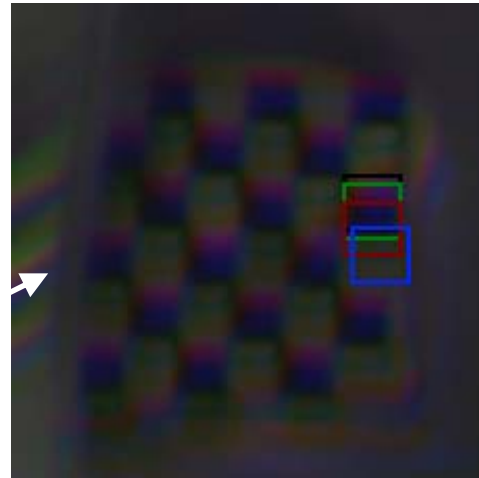
Fig. C3b: The coloured squares display how much the target has moved (black: 10 ms, equal to 0 ms, green: 15 ms, red = 20 ms, blue = 25 ms).
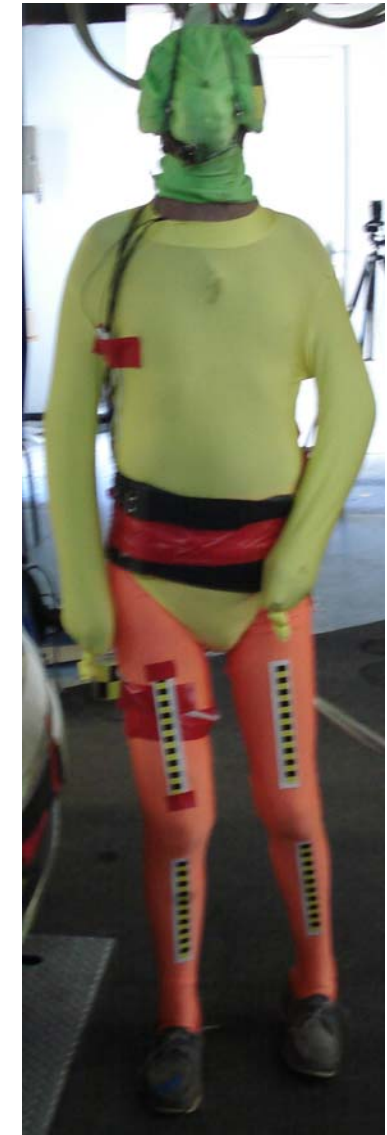
Fig. C4: Pre-test posture. The legs are slightly angled; the right foot is approximately 10 cm in front of the left foot. The feet are approximately 12 cm apart.

Appendix D: Accident data

TABLE D-I
Accident Data
Deviation from 100 % is due to rounding.

Number of cases	total		shoulder impact		elbow impact		head impact	
	Absolute number	% of all	Absolute number	% of subset	Absolute number	% of subset	Absolute number	% of subset
Vehicle speed unknown (cases)	108	9	10	5	7	6	17	4
Speed (km/h)	29 ± 17	-	35 ± 16	-	29 ± 13	-	38 ± 17	-
MAIS 0-2 (cases)	960	79	148	73	92	80	271	66
MAIS 3-4 (cases)	128	11	32	16	15	13	76	18
MAIS 5-6 (cases)	36	3	10	5	4	3	29	7
MAIS 9 (cases)	88	7	13	6	4	3	36	9
Fatal cases	51	4	12	6	6	5	42	10
Non-fatal cases	1161	96	191	94	109	95	370	90
Pedestrian hit laterally (cases)	837	69	148	73	86	75	308	75
Ped. hit almost laterally (cases)	139	11	19	9	13	11	38	9
Other impact directions (*)	178	15	29	14	14	12	55	13
Impact direction unknown (cases)	58	5	7	3	2	2	11	3
Shoulder impact (cases)	203	17	203	100	28	24	120	29
No shoulder impact (cases)	937	77	-	-	82	71	272	66
Unknown if shoulder impact (cases)	72	6	-	-	5	4	20	5
Elbow impact (cases)	115	9	28	14	115	100	43	10
No elbow impact (cases)	1033	85	169	83	-	-	355	86
Unknown if elbow impact (cases)	64	5	6	3	-	-	14	3
Head impact (cases)	412	34	120	59	43	37	412	100
No head impact (cases)	749	62	83	41	68	59	-	-
Unknown if head impact (cases)	51	4	0	0	4	3	-	-
Head WAD unknown (cases)	891	74	108	53	84	73	99	24
Head WAD (cm)	186 ± 43	-	195 ± 43	-	180 ± 48	-	187 ± 43	-
Ped. size unknown (cases)	314	26	52	26	26	23	119	29
Ped. size (cm)	160 ± 20	-	166 ± 17	-	161 ± 20	-	163 ± 19	-
Head WAD or size unknown (cases)	970	80	125	62	90	78	177	43
Head WAD/size ratio	1.13 ± 0.22	-	1.15 ± 0.24	-	1.06 ± 0.23	-	1.13 ± 0.22	-
total	1212	100	203	100	115	100	412	100

(*) Pedestrians facing the vehicle or being hit from behind (impact direction 11-1 o'clock and 5-7 o'clock).